SPECIAL
CAHMDA III
COLLECTION

# Parameter Sensitivity in LSMs: An Analysis Using Stochastic Soil Moisture Models and ELDAS Soil Parameters

ADRIAAN J. TEULING

*ETH Zurich, Zurich, Switzerland*

REMKO UIJLENHOET

*Wageningen University, Wageningen, Netherlands*

BART VAN DEN HURK

*Royal Netherlands Meteorological Institute (KNMI), De Bilt, Netherlands*

SONIA I. SENEVIRATNE

*ETH Zurich, Zurich, Switzerland*

## ABSTRACT

Integration of simulated and observed states through data assimilation as well as model evaluation requires a realistic representation of soil moisture in land surface models (LSMs). However, soil moisture in LSMs is sensitive to a range of uncertain input parameters, and intermodel differences in parameter values are often large. Here, the effect of soil parameters on soil moisture and evapotranspiration are investigated by using parameters from three different LSMs participating in the European Land Data Assimilation System (ELDAS) project. To prevent compensating effects from other than soil parameters, the effects are evaluated within a common framework of parsimonious stochastic soil moisture models. First, soil parameters are shown to affect soil moisture more strongly than the average evapotranspiration. In arid climates, the effect of soil parameters is on the variance rather than the mean, and the intermodel flux differences are smallest. Soil parameters from the ELDAS LSMs differ strongly, most notably in the available moisture content between the wilting point and the critical moisture content, which differ by a factor of 3. The ELDAS parameters can lead to differences in mean volumetric soil moisture as high as 0.10 and an average evapotranspiration of 10%–20% for the investigated parameter range. The parsimonious framework presented here can be used to investigate first-order parameter sensitivities under a range of climate conditions without using full LSM simulations. The results are consistent with many other studies using different LSMs under a more limited range of possible forcing conditions.

## 1. Introduction

The dynamic role of the land surface in the climate system is nowadays widely recognized. Fluxes of latent heat from the land surface into the atmosphere transport large amounts of energy and water and limit direct heating of the lower atmosphere. Their magnitude, however, strongly depends on the soil moisture content of the soil. Model studies have shown that without soil moisture interacting freely with the atmosphere, warm season precipitation and temperature variability over land are significantly reduced (e.g., Douville 2003; Koster et al. 2004; Seneviratne et al. 2006a). It is also known that there is a tight relation between soil moisture and screen-level temperature and humidity (Mahfouf 1991). In addition, there is a two-way coupling between the memory of the land surface and the strength of the coupling between the land surface and the atmosphere (Koster and Suarez 1996, 2001).

*Corresponding author address:* Adriaan J. Teuling, Institute for Atmospheric and Climate Science, CHN N 16.2, Universitätstrasse 16, 8092 Zurich, Switzerland.
E-mail: ryan.teuling@env.ethz.ch

The correct simulation of land surface–atmosphere interactions requires the realistic representation of both soil moisture and evapotranspiration. Unfortunately, current land surface models (LSMs) depend on many uncertain parameters; as a result, they strongly differ on both soil moisture and evapotranspiration (e.g., Lohmann and Wood 2003; Teuling et al. 2006), with consequent divergence in land–atmosphere coupling strength (e.g., Koster et al. 2004) or persistence patterns (e.g., Seneviratne et al. 2006b).

The uncertainty in many LSM parameters combined with the high sensitivity of simulated states and fluxes to these parameters can cause spurious drifts in the soil moisture state. To address this issue in model-based soil moisture products, different land data assimilation systems have been developed to constrain simulated soil moisture to observations of screen-level temperature and humidity (e.g., Bouttier et al. 1993; Rhodin et al. 1999; Douville et al. 2000), surface soil moisture or surface emissivity (e.g., Heathman et al. 2003; Galantowicz et al. 1999; Reichle and Koster 2005), latent heat fluxes (e.g., van den Hurk et al. 1997; Schuurmans et al. 2003), or to a combination of these (e.g., Seuffert et al. 2003).

While data assimilation provides a pragmatic solution to momentarily improve soil moisture states, later biases are not prevented since most data assimilation approaches deal with model states rather than parameters (in contrast to calibration). In fact, many data assimilation techniques assume bias-free models as well as observations. In addition, some data assimilation schemes (especially in reanalysis data products) mostly aim at an improvement of the turbulent fluxes through the soil moisture increments. As a consequence, some soil moisture assimilation schemes may even lead to a deterioration of the soil moisture fields (e.g., Betts et al. 2003; Seneviratne et al. 2004). Calibration of soil parameters to effective rather than physical values improves soil moisture data, but observations at larger scales are scarce (Ines and Mohanty 2008). To effectively prevent, or even reduce, soil moisture biases, improvements in model parameterization are thus needed (Jacobs et al. 2008).

Soil parameters control the storage capacity and loss rates of the soil per unit depth; hence they affect the simulation of soil moisture and evapotranspiration in LSMs. The variability in soil parameters within different textural classes often exceeds the variability between the classes (Soet and Stricker 2003; Gutmann and Small 2006), likely resulting in large differences between LSMs that derive their parameters from different soil databases. Also, the exact magnitude of this effect is uncertain. Some studies report a high sensitivity of both soil moisture and evapotranspiration to soil characteristics, such as the water-holding capacity or other soil

hydraulic properties (e.g., Soet et al. 2000; Seneviratne et al. 2006b), while others reported mainly an effect on soil moisture (Richter et al. 2004; Braun and Schädler 2005; Kato et al. 2007). The sensitivity of a LSM to its parameters also depends on the climate conditions (e.g., Pitman 1994; Bastidas et al. 1999; Soet et al. 2000; Liang and Guo 2003; Kahan et al. 2006). A general framework that can help to understand why these sensitivities to soil parameters differ between models and climates is currently lacking.

In this study, we investigate the potential, or isolated, effect of soil parameters (e.g., wilting point, porosity, saturated hydraulic conductivity) on soil moisture and the mean water budget components under stochastic forcing. Here, potential means that the soil parameters are isolated from their original model, and their effect is evaluated using a parsimonious framework of stochastic soil moisture models. Through this methodology, we only evaluate the effect of parameters from different LSMs, not the LSMs themselves. Also, model-dependent compensating effects as a result of parameter interactions (see, e.g., Liang and Guo 2003) are avoided. Finally, the results are obtained under statistical steady-state conditions. While sensitivity studies with full LSMs require specification of initial and transient forcing conditions (which are typically far from being steady state), the results obtained with our current approach are independent of both. Therefore, they are likely to be more general.

The stochastic models are of considerably lower complexity than the full LSMs. Nonetheless, their equations for the soil moisture dependency on evapotranspiration and drainage are the same, or at least very similar. Indeed, it has been shown that just by using the point-specific linearized dependencies of evapotranspiration and drainage to soil moisture, most of the grid-point soil moisture variability in original LSMs can be reproduced (Koster and Milly 1997). While stochastic soil moisture models have mainly been used for theoretical analysis (e.g., Rodríguez-Iturbe and Porporato 2004), they have also been applied to describe soil moisture observations in regions with either strong or weak seasonality in forcing (e.g., Calanca 2004; Teuling et al. 2005; Miller et al. 2007; Teuling et al. 2007). The stochastic models are described in section 2.

Soil parameters are taken from three LSMs used within the European Land Data Assimilation System project (ELDAS). For more information on the ELDAS soil moisture, we refer to Jacobs et al. (2008) and van den Hurk et al. (2008). The ELDAS LSMs differ widely in their treatment of the parameters governing the soil water balance, and they are likely to be representative for the whole range of operational LSMs. The soil

parameterizations of the ELDAS models are described in section 3. It should be noted that some LSM parameters are calibrated to optimize a particular model's performance, and their conceptual rather than physical meaning would prohibit direct intercomparison. This is, however, not the case for soil parameters. Their values are often derived from observations and are assigned to LMSs as attributes of soil textural classes.

## 2. Stochastic soil moisture models

### a. General outline

For a single-layer model with effective depth of the root zone $d_{rz}$, temporal changes in the volumetric water content $\theta$ or the saturation degree $s$ can be expressed as

$$\frac{d\theta}{dt} = \frac{1}{d_{rz}}(P - I - R - \text{ET} - Q) \quad \text{and} \quad (1a)$$

$$\frac{ds}{dt} = \frac{1}{\theta_s d_{rz}}(P - I - R - \text{ET} - Q), \quad (1b)$$

where $P$ is the precipitation, $I$ is the rate of interception by leaves, $R$ is the saturation excess runoff, ET is the total evapotranspiration (through root water uptake and soil evaporation), $Q$ is the drainage from the base of the soil profile, and $\theta_s$ is the soil moisture content at saturation (porosity). In what follows, we will use both $\theta$ and $s$, depending on which is more convenient. Although Eq. (1) is not solved directly, it is implicitly considered in the steady-state probability distributions of soil moisture used in this study. Since we focus on the effect of soil parameters rather than root depth, we will use a constant $d_{rz}$ of 600 mm, though the effect of $\pm 10\%$ changes in $d_{rz}$ are also investigated hereafter. For all vegetation types, the bulk of the roots is present above this depth (Schenk and Jackson 2002). Next, the parameterization of different water balance components and their relation to land surface characteristics are described.

### b. Evapotranspiration losses

Water extraction from soils for transpiration in common "biophysical" LSMs (Sellers et al. 1997) is generally driven by the bulk exchange formula for latent heat, with additive aerodynamic resistance $r_a$ and canopy resistance $r_c$:

$$\text{ET} = \frac{\rho_a}{\rho_w} \cdot \frac{\Delta q}{r_a + r_c}, \quad (2)$$

where $\rho_a$ is the density of air, $\rho_w$ is the density of water, and $\Delta q$ is the specific humidity gradient between the surface and the lowest atmospheric level. Here, we assume a typical value of $r_a = 10$ s m$^{-1}$ (Sellers et al.

1997). The canopy or surface resistance $r_c$ is a function of a minimum (unstressed) stomatal resistance $r_{s,\min}$, the leaf area index LAI, and a (model dependent) number $m$ of environmental stress functions $f_i$ depending on factors such as temperature, radiation, or soil moisture:

$$r_c = \frac{r_{s,\min}}{\text{LAI}} \prod_{i=1}^{n} f_i. \quad (3)$$

Here, we use $r_{s,\min} = 150$ s m$^{-1}$ and LAI $= 3$. These values are typical for low, fully developed vegetation, such as grass and crops (van den Hurk et al. 2000). Only the effect of the soil moisture reduction function $f(\theta)$ is considered here, and the effect of day-to-day variations of vapor pressure deficit and photosynthetic active radiation effects on $r_c$ (see Jarvis 1976) are neglected. As a result, only systematic longer term (multiday) changes in ET as a result of the depletion of the soil moisture reservoir are accounted for, such as those analyzed by Teuling et al. (2006). The function $f(\theta)$ is generally nonlinear and is often expressed as (e.g., Sellers et al. 1997; van den Hurk et al. 2000; Albertson and Kiely 2001)

$$f(\theta)^{-1} = \begin{cases} 0, & \theta \leq \theta_w \\ \dfrac{\theta - \theta_w}{\theta_c - \theta_w}, & \theta_w < \theta \leq \theta_c, \\ 1, & \theta_c < \theta \leq \theta_s \end{cases} \quad (4)$$

where $\theta_w$ is the permanent wilting point and $\theta_c$ is the critical moisture content below which stomatal opening is reduced as a result of soil moisture stress. To ensure a (bi)linear relation between ET and $\theta$ for compatibility with the analytical solutions of Rodríguez-Iturbe et al. (1999) and Laio et al. (2001), we apply $f(\theta)^{-1}$ directly to the maximum unstressed ET (e.g., Sellers et al. 1997; Albertson and Kiely 2001):

$$\text{ET}(\theta) = f(\theta)^{-1} \frac{\rho_a}{\rho_w} \frac{\Delta q}{r_a + \frac{r_{s,\min}}{\text{LAI}}} = f(\theta)^{-1} \text{ET}_{\max}. \quad (5)$$

In the following equation, we will refer to $\text{ET}_{\max}$ as the (constant) rate of ET whenever soil moisture is not limiting. Some models also allow for soil moisture drying below $\theta_w$. We accommodate for this by $E_w$, a residual soil evaporation at $\theta_w$ that linearly reduces to zero toward the residual moisture content $\theta_r$ ($\theta_r < \theta_w$, see Fig. 1).

The temporal average ET can be obtained by the integration of the functional relation between $\theta$ and ET, with the corresponding probability density distribution $p(\theta)$ that results from the stochastic rainfall forcing:

$$\langle \text{ET} \rangle = \int_{\theta_r}^{\theta_s} \text{ET}(\theta) p(\theta) d\theta. \quad (6)$$
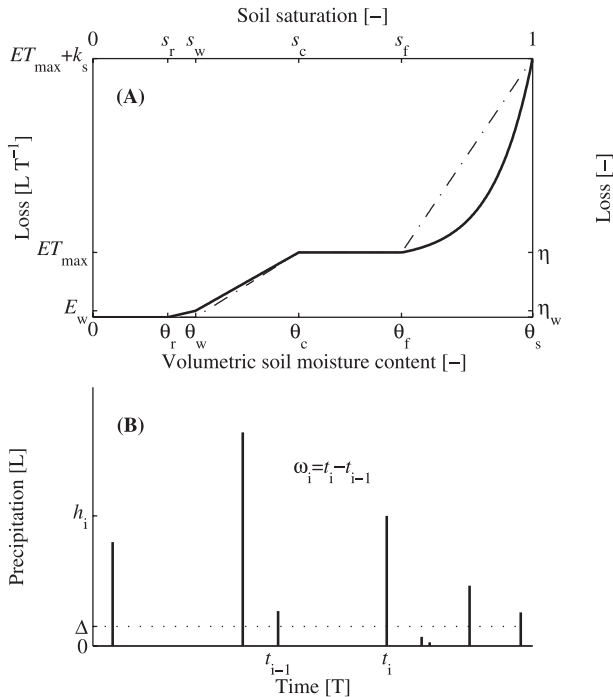
FIG. 1. Definition of variables. (a) Loss function and associated variables for the (bottom $x$ axis) regular and the (top $x$ axis) dimensionless notation and for linear [Eq. (8), dash–dotted line] and nonlinear [Eq. (9), solid line] drainage. (b) Stochastic precipitation process. Here, the canopy storage $\Delta$ acts as a threshold for the rainfall, effectively reducing the mean storm arrival rate $\lambda$ but not the mean storm depth $\alpha$ [Eq. (13)]. Note that in general, $k_s$ is several orders of magnitude larger than $ET_{max}$.

This equation has been used in previous studies to assess the effect of spatial, rather than temporal, soil moisture distributions on the spatially average ET (e.g., Crow and Wood 2002; Sellers et al. 2007).

### c. Drainage losses

In reality, the water flux at the base of the root zone is determined both by gravitational forces and additional capillary forces as a result of the presence of groundwater (Bogaart et al. 2008). In LSMs, capillary effects are often neglected (Albertson and Kiely 2001). In this case, the flux equals the hydraulic conductivity at the given moisture content, that is, $Q = k(\theta)$, where the moisture content is that of the deepest model layer. Many models use the power law function to describe the dependency of the hydraulic conductivity $k$ on $\theta$ (e.g., Clapp and Hornberger 1978):

$$k(\theta) = k_s \left(\frac{\theta}{\theta_s}\right)^{2b+3} \Leftrightarrow k(s) = k_s s^{2b+3}, \quad (7)$$

where $k_s$ is the saturated hydraulic conductivity and $b$ is a retention parameter. In other cases, the nonlinear $k(\theta)$

relation is approximated by a piecewise linear function (e.g., Rodríguez-Iturbe et al. 1999):

$$k(s) = k_s \frac{s - s_f}{1 - s_f}, \quad s_f < s \leq 1, \quad (8)$$

where the field capacity $s_f$ is chosen such that the best fit is obtained with Eq. (7). For reasons of mathematical tractability, Laio et al. (2001) proposed the following exponential function to fit Eq. (7):

$$k(s) = k_s \frac{e^{\beta(s-s_f)} - 1}{e^{\beta(1-s_f)} - 1}, \quad s_f < s \leq 1, \quad (9)$$

where $\beta$ is related to $b$ [Eq. (7)] as $\beta = 2b + 4$ [refer to Laio et al. (2001) for details]. Note that in contrast to Eq. (7), Eqs. (8) and (9) assume that water movement below $\theta_f$ can be neglected. Similar to Eq. (6), the temporal average drainage $\langle Q \rangle$ is given by

$$\langle Q \rangle = \int_{\theta_f}^{\theta_s} Q(\theta) p(\theta) d\theta. \quad (10)$$

The relation between the combined drainage and evapotranspiration losses and the soil moisture state is the so-called loss function, and is shown in Fig. 1 for both Eqs. (8) and (9).

### d. Infiltration and runoff

Precipitation is an intermittent process; therefore, we include a stochastic representation of rainfall pulses in the model that accounts for alternating wetting and drying events under given climate conditions and yet preserves the possibility of analytical solutions. Here, rainstorms occur instantaneously and are represented by a marked Poisson process. The distribution of time $\omega_i$ between two successive storms at $t_i$ and $t_{i+1}$ and the depth $h_i$ of an individual storm at $t_i$ are independent random variables (Fig. 1). Their distributions are exponential:

$$p(\omega) = \lambda e^{-\lambda \omega}, \quad \omega \geq 0 \quad \text{and} \quad (11)$$

$$p(h) = \frac{1}{\alpha} e^{-h/\alpha}, \quad h \geq 0, \quad (12)$$

where $\lambda$ is the mean storm arrival rate and $\alpha$ is the mean storm depth. If part of the rainfall is intercepted by a canopy reservoir with capacity $\Delta$ (here 0.5 mm) and no memory, the infiltration becomes a new (censored) marked Poisson process (Laio et al. 2001), with a reduced mean storm arrival rate $\lambda' = \lambda \exp(-\Delta/\alpha)$. Since $\langle P \rangle = \alpha \lambda$, the resulting mean interception rate of the process is

$$\langle I \rangle = \alpha(\lambda - \lambda'). \quad (13)$$

It is assumed that runoff occurs only whenever the depth of a rainfall event exceeds the available storage. Figure 2 shows an illustration of the stochastic forcing and the resulting temporal soil moisture evolution.

## e. Steady-state distributions

In the case of piecewise linear losses [i.e., evapotranspiration using Eq. (5) and linear drainage of Eq. (8)], an analytical solution of the steady-state soil moisture probability density function (hereafter pdf) was derived by Rodríguez-Iturbe et al. (1999). For notational convenience, we follow Rodríguez-Iturbe et al. (1999) and express the pdf $p$ in terms of soil wetness $s = \theta/\theta_s$:
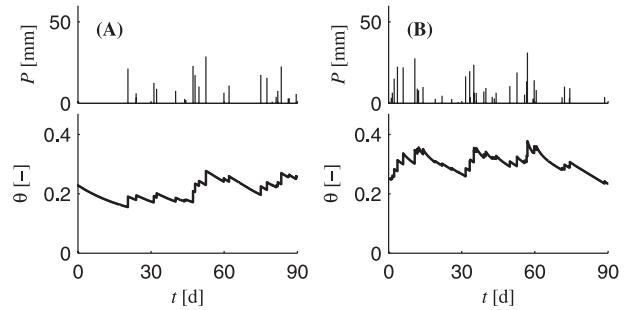


FIG. 2. Illustration of the (top) marked Poisson rainfall process ($P$) and (bottom) resulting traces of soil moisture ($\theta$) for the (a) arid and (b) humid climates. Note that in the arid climate, soil moisture losses generally occur at a lower rate.

$$p(s) = \begin{cases} \dfrac{C_1}{\eta}\left(\dfrac{s-s_w}{s_c-s_w}\right)^{[\lambda'(s_c-s_w)/\eta]-1} e^{-\gamma s}, & 0 < s \le s_c, \\[3mm] \dfrac{C_1}{\eta}\exp\left(-\dfrac{\lambda's_c}{\eta}\right)\exp\left[-s\left(\gamma-\dfrac{\lambda'}{\eta}\right)\right], & s_c < s \le s_f, \\[3mm] \dfrac{C_1}{\eta}\left[\dfrac{k(s-s_f)}{(1-s_f)\eta}+1\right]^{[\lambda'(1-s_f)/k]-1}\exp\left(-\gamma s+\lambda'\dfrac{s_f-s_c}{\eta}\right), & s_f < s \le 1, \end{cases} \tag{14}$$

where $\eta = \mathrm{ET}_{\max}/\theta_s d_{rz}$, $\gamma = \theta_s d_{rz}/\alpha$, and $C_1$ is an integration constant. Next, we consider the case of nonlinear drainage losses [Eq. (9)] combined with a residual soil evaporation $E_w$ for $\theta < \theta_w$. In this case, the steady-state distribution $p(s)$ becomes (Laio et al. 2001)

$$p(s) = \begin{cases} \dfrac{C_2}{\eta_w}\left(\dfrac{s-s_r}{s_w-s_r}\right)^{\frac{\lambda'(s_w-s_r)}{\eta_w}-1}e^{-\gamma s}, & s_r < s \le s_w, \\[3mm] \dfrac{C_2}{\eta_w}\left[1+\left(\dfrac{\eta}{\eta_w}-1\right)\left(\dfrac{s-s_w}{s_c-s_w}\right)\right]^{\frac{\lambda'(s_c-s_w)}{\eta-\eta_w}-1}e^{-\gamma s}, & s_w < s \le s_c, \\[3mm] \dfrac{C_2}{\eta}e^{-\gamma s+\frac{\lambda'}{\eta}(s-s_c)}\left(\dfrac{\eta}{\eta_w}\right)^{\lambda'\frac{s_c-s_w}{\eta-\eta_w}}, & s_c < s \le s_f, \\[3mm] \dfrac{C_2}{\eta}e^{-(\beta+\gamma)s+\beta s_f}\left[\dfrac{\eta e^{\beta s}}{(\eta-m)e^{\beta s_f}+m e^{\beta s}}\right]^{\frac{\lambda'}{\beta(\eta-m)}+1}\left(\dfrac{\eta}{\eta_w}\right)^{\lambda'\frac{s_c-s_w}{\eta-\eta_w}}e^{\frac{\lambda'}{\eta}(s_f-s_c)}, & s_f < s \le 1, \end{cases} \tag{15}$$

where $\eta_w = E_w/\theta_s d_{rz}$, $\gamma = \theta_s d_{rz}/\alpha$, and $m$ is given by

$$m = \frac{k_s}{\theta_s d_{rz}[e^{\beta(1-s_f)}-1]}. \tag{16}$$

The integration constants $C_1$ and $C_2$ in Eqs. (14) and (15) can be obtained by imposing the condition

$$\int_{\theta_r}^{\theta_s} p(\theta)\,d\theta = 1. \tag{17}$$

For the pdfs given by Eqs. (14) and (15), no easy expression exists for the moments (i.e., mean and variance). To this end, a useful simplification can be made

by assuming that the losses, which are linear between $\theta_w$ and $\theta_c$, maintain the same slope also above $\theta_c$. This assumption is only appropriate for the arid climate, where soil moisture excursions above $\theta_c$ are rare. Here, the time scale $\tau = d_{rz}(\theta_c - \theta_w)/\mathrm{ET}_{\max}$ of the exponential decay in ET resulting from drying between $\theta_c$ and $\theta_w$ is of particular interest, since this can be used to infer land surface properties from ET observations (Teuling et al. 2006). In this case, the steady-state distribution is a shifted gamma distribution (Teuling et al. 2007):

$$p(\theta) = \frac{(\theta-\theta_w)^{\lambda'\tau-1}\exp\left(-\dfrac{\theta-\theta_w}{c}\right)}{c^{\lambda'\tau}\Gamma(\lambda'\tau)}, \quad \theta \ge \theta_w, \tag{18}$$
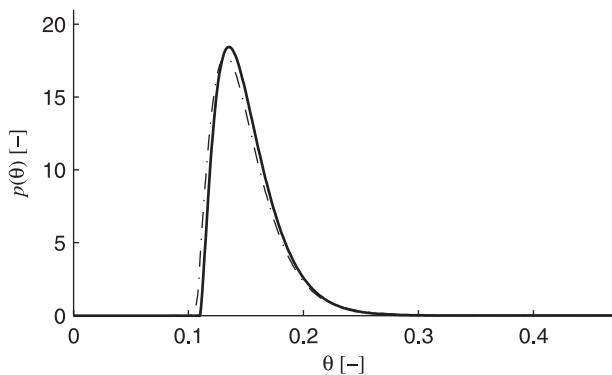
FIG. 3. Steady-state soil moisture distributions $p(\theta)$ for the arid climate. Thick line is the shifted gamma distribution. Dash–dotted line is the Laio et al. (2001) model. Both have the same parameter values.

TABLE 1. Climate characteristics for the typical arid, transitional, and humid climates used in this study.

| | Arid | Transitional | Humid |
|---|---|---|---|
| Mean storm arrival rate $\lambda$ (day$^{-1}$) | 0.2 | 0.4 | 0.5 |
| Mean storm depth $\alpha$ (mm) | 10.0 | 10.0 | 10.0 |
| Potential evapotranspiration ET$_{max}$ (mm day$^{-1}$) | 5.00 | 4.00 | 3.00 |
| Mean precipitation rate $\langle P \rangle$ (mm day$^{-1}$) | 2.00 | 4.00 | 5.00 |
| Mean interception rate $\langle I \rangle$ (mm day$^{-1}$) | 0.10 | 0.20 | 0.24 |
| Net infiltration $\langle P \rangle - \langle I \rangle$ (mm day$^{-1}$) | 1.90 | 3.80 | 4.76 |

where $c = \alpha/d_{rz}$. The validity of the linear-loss simplification under arid climate conditions is shown in Fig. 3, where it is shown that the gamma distribution is in good agreement with the more complex Laio et al. (2001) model [Eq. (15)]. The gamma distribution Eq. (18) has mean

$$\langle \theta \rangle = \theta_w + \lambda' \tau c \qquad (19)$$

and variance Var $(\theta)$ proportional to $\tau$:

$$\text{Var}(\theta) = \lambda' \tau c^2, \qquad (20)$$

so that with all other parameters constant, $\text{Var}(\theta) \propto \theta_c - \theta_w$. Since $\text{ET} = (\theta - \theta_w)d_{rz}/\tau$, the mean evapotranspiration equals the mean infiltration: $\langle \text{ET} \rangle = \lambda' \alpha$. By using $\text{Var(ET)} = \text{Var}(\theta)d_{rz}^2/\tau^2$, it follows that $\text{Var(ET)}$ is inversely proportional to the retention time scale $\tau$:

$$\text{Var(ET)} = \frac{\lambda' \alpha^2}{\tau}, \qquad (21)$$

so that $\text{Var(ET)} \propto (\theta_c - \theta_w)^{-1}$.

### f. Climate conditions

Here, we will consider three different climatic conditions for simplicity: "humid," "arid," and "transitional." Evapotranspiration in the humid climate is limited by the supply of energy. Potential evapotranspiration rates are relatively moderate as a result of higher humidity, lower temperatures, and lower net radiation, and the average infiltration exceeds the potential (unstressed) evapotranspiration: $\langle P \rangle - \langle I \rangle > \text{ET}_{max}$. In contrast, evapotranspiration is limited by the availability of soil moisture in the arid climate. Here, potential evapotranspiration exceeds the average infiltration:

$\text{ET}_{max} > \langle P \rangle - \langle I \rangle$. In the transitional climate, the average infiltration is balanced by $\text{ET}_{max}$, so that $\text{ET}_{max} \approx \langle P \rangle - \langle I \rangle$. The average specific humidity gradient $\Delta q$ is chosen such that $\text{ET}_{max}$ equals 3, 4, and 5 mm day$^{-1}$ for the humid, transitional, and arid climate, respectively. The forcing is listed in Table 1. Figure 2 shows forcing realizations for the humid and arid climates, along with the resulting soil moisture.

### g. Parameter sensitivity

Since no easy expression exists for the mean and variance of Eq. (15), we evaluate the sensitivity of soil moisture to the different parameters by looking at the pdf directly. The rationale behind this is that if changing any parameter affects soil moisture, this will also affect $p(\theta)$. Or, alternatively, if $p(\theta)$ does not change in response to a parameter perturbation, soil moisture has no sensitivity to this parameter. We will investigate the sensitivity to equal (namely, 10%) parameter perturbations, so that the relative (or normalized) effect can be directly compared. One should note that the actual uncertainty range is parameter dependent and that a 10% range can be too optimistic, especially for parameters that are known to vary over orders of magnitude (such as $k_s$). For most parameters, however, realistic confidence intervals are unknown.

From a land surface modeling perspective, the key interest might be in $\langle \text{ET} \rangle$ rather than soil moisture. Since analytical expressions for $\langle \text{ET} \rangle$ and its sensitivity to the different parameters cannot be easily obtained, this is investigated numerically. For any parameter $\Pi$, the relative sensitivity $\sigma$ of $\langle \text{ET} \rangle$ to $\Pi$ can be approximated by

$$\sigma = \frac{\Pi}{\langle \text{ET} \rangle} \frac{\Delta\langle \text{ET} \rangle}{\Delta\Pi}, \qquad (22)$$

where $\Delta\langle \text{ET} \rangle$ is the range in $\langle \text{ET} \rangle$, resulting from a small parameter perturbation $\Delta\Pi$ (here 1%).

TABLE 2. Soil parameters of the three LSMs used within the ELDAS project, and the mean soil moisture $\langle\theta\rangle$ for the arid climate. Columns are merged when there is no functional difference between two parameters.

| Soil texture | $\theta_r$ | $\theta_w$ | $\theta_c$ | $\theta_f$ | $\theta_s$ | $k_s$ (mm day$^{-1}$) | $\theta_c - \theta_w$ | $\langle\theta\rangle$ |
|---|---|---|---|---|---|---|---|---|
| Reference | 0.080 | 0.110 | 0.220 | 0.290 | 0.470 | 400 | | |
| | | | TERRA parameters | | | | | |
| Sand | 0.012 | 0.042 | 0.167 | 0.196 | 0.364 | 4138 | 0.125 | 0.091 |
| Sandy loam | 0.030 | 0.100 | 0.230 | 0.260 | 0.445 | 815 | 0.130 | 0.151 |
| Loam | 0.035 | 0.110 | 0.293 | 0.340 | 0.455 | 459 | 0.186 | 0.184 |
| Loamy clay | 0.060 | 0.185 | 0.335 | 0.370 | 0.475 | 66 | 0.150 | 0.244 |
| Clay | 0.065 | 0.257 | 0.424 | 0.463 | 0.507 | 1 | 0.167 | 0.323 |
| Peat | 0.098 | 0.265 | 0.668 | 0.763 | 0.863 | 5 | 0.403 | 0.424 |
| | | | (H)TESSEL parameters | | | | | |
| Coarse | 0.025 | 0.059 | 0.244 | | 0.403 | 600 | 0.185 | 0.129 |
| Medium | 0.010 | 0.151 | 0.347 | | 0.439 | 100 | 0.196 | 0.226 |
| Medium (TESSEL) | 0.171 | | 0.323 | | 0.472 | 395 | 0.152 | 0.229 |
| Medium fine | 0.010 | 0.133 | 0.383 | | 0.430 | 22 | 0.250 | 0.228 |
| Fine | 0.010 | 0.279 | 0.448 | | 0.520 | 248 | 0.169 | 0.343 |
| Very fine | 0.010 | 0.335 | 0.541 | | 0.614 | 150 | 0.206 | 0.413 |
| Organic | N/A | 0.267 | 0.663 | | 0.766 | 80 | 0.396 | 0.418 |
| | | | ISBA parameters | | | | | |
| Sand | 0.083 | | 0.156 | | 0.397 | 497 | 0.073 | 0.111 |
| Sandy loam | 0.117 | | 0.199 | | 0.430 | 241 | 0.082 | 0.149 |
| Loam | 0.166 | | 0.254 | | 0.451 | 117 | 0.088 | 0.199 |
| Loamy clay | 0.220 | | 0.309 | | 0.462 | 65 | 0.089 | 0.254 |
| Clay | 0.288 | | 0.373 | | 0.473 | 37 | 0.085 | 0.320 |

## h. ELDAS Soil parameters

### 1) TESSEL AND HTESSEL

Tiled ECMWF Scheme for Surface Exchanges over Land has been developed at the European Centre for Medium Range Weather Forecasts (ECMWF). In the original version of TESSEL, only one soil type exists. The physical properties of this soil (Table 2) were chosen, such that the water-holding capacity of 1 m of soil is approximately 15 cm (see Viterbo and Beljaars 1995), corresponding to the water-holding capacity of the original Bucket model (Manabe 1969). Gravitational drainage from the lowest layer is calculated from Eq. (7). Evapotranspiration is reduced for $\theta < \theta_f$, so that there is no distinction between $\theta_c$ and $\theta_f$. The recent version of TESSEL, HTESSEL, has improved hydrology and distinguishes between six different soil types, each with its own parameters. Here, (H)TESSEL refers to both models.

### 2) ISBA

Interactions between Soil, Biosphere, and Atmosphere have been developed at the Centre National de Recherches Météorologiques (CNRM), Météo-France. In ISBA, the $\theta_w$, $\theta_f$, and $\theta_s$ are calculated from continuous pedotransfer functions based on the percentages of sand and clay. The formulas are (Noilhan and Mahfouf 1996)

$$\theta_w = 37.1342 \times 10^{-3}(\text{CLAY})^{0.5}, \tag{23a}$$

$$\theta_f = 89.0467 \times 10^{-3}(\text{CLAY})^{0.3496}, \quad \text{and} \tag{23b}$$

$$\theta_s = (-1.08\,\text{SAND} + 494.305) \times 10^{-3}, \tag{23c}$$

where CLAY and SAND are the percentages of clay and sand, respectively. There is no organic soil type. Drainage is assumed to take place only above $\theta_f$ and is a linear function of the soil moisture content above $\theta_f$ following the approach of Mahfouf and Noilhan (1996):

$$Q = C_3 \frac{d_{rz}}{\tau_1}(\theta - \theta_f), \quad \theta \geq \theta_f, \tag{24}$$

where $\tau_1$ is a restore constant ($= 1$ day). Note the similarity with Eq. (8). The constant $C_3$ is calculated from [refer to Mahfouf and Noilhan (1996) for details]

$$C_3 = \frac{\tau_1(2b + 2)k_s}{d_{rz}\theta_s[(\theta^*/\theta_s)^{-2b-2} - 1]}, \tag{25}$$

where $\theta^*$ is the soil moisture content at a fraction of $1/e$ going from $\theta_f$ to $\theta_s$. Alternatively, $C_3$ can be determined from the following regression with CLAY (Noilhan and Mahfouf 1996):

$$C_3 = 5.327 \times \text{CLAY}^{-1.043}. \tag{26}$$

Although, strictly speaking, the difference between linear and nonlinear drainage is a matter of parameterization rather than parameters, we will include the effect of linear drainage in the study, since $C_3$ is an effective parameter defined only for linear drainage. For comparison with the discrete soil classes of the other two models, we adopt values for CLAY of 5%, 10%, 20%, 35%, and 60% for typical sand, sandy loam, loam, loamy clay, and clay soils, respectively; for SAND, we use corresponding values of 90%, 60%, 40%, 30%, and 20%, respectively. Because of the linear nature of the force–restore drainage [Eq. (24)] in ISBA and the absence of ET below $\theta_w$, we use Eq. (14) rather than Eq. (15) to assess the effect of ISBA soil parameters. The resulting values using Eqs. (23) and (26) are listed in Table 2.

### 3) TERRA

TERRA was developed at the German Weather Service (DWD). In TERRA, six different soil classes are distinguished (excluding ice and rock). Most of the soil parameters ($\theta_r$, $\theta_w$, $\theta_f$, $\theta_s$, and $k_s$) are listed in a lookup table for each soil class (Table 2). The critical moisture content $\theta_c$, however, is calculated dynamically as a function of $ET_{max}$ following Denmead and Shaw (1962):

$$\theta_c = \theta_w + (\theta_f - \theta_w)[0.81 + 0.121 \arctan \times (ET_{max} - ET_{max,norm})], \quad (27)$$

where $ET_{max,norm} = 4.75$ mm day$^{-1}$. TERRA also distinguishes between the permanent wilting point $\theta_w$ and the hygroscopic or residual point $\theta_r$, below which the remaining water is bound to the soil particles.

## 3. Results

### a. Model sensitivity

First, we discuss the sensitivity of soil moisture and ET to the model parameters in the most complex Laio et al. (2001) model [Eq. (15)] using average parameters corresponding to a typical loamy soil (Table 2). Figure 4 shows the perturbation in $p(\theta)$ resulting from equal (10%) perturbations in all parameters (including forcing) for the three climates. The gray areas in the figure correspond to the outer envelope of pdfs resulting from the parameter perturbation—that is, the gray area contains all possible pdfs within the ±10% parameter range.

It can be seen in Fig. 4 that soil moisture is not equally sensitive to all parameters and that the sensitivity also depends on climate. Any perturbation in parameters that are associated with small water fluxes ($\theta_r$, $E_w$, $\Delta$) is hardly reflected in $p(\theta)$ (Figs. 4a, 4f, and 4i). As can be expected, soil parameters that regulate the soil moisture reduction on ET ($\theta_w$, $\theta_c$) have an effect on soil moisture in the arid and transitional climates but not in the humid climate, where ET is not limited by soil moisture. Similarly, soil parameters that control drainage ($\theta_f$, $\theta_s$, $b$, and $k_s$) effect soil moisture in the humid and transitional climates but not in the arid climate. Because of the nonlinearity in drainage [Eq. (9)], a relative change in $\theta_f$ or $\theta_s$ has a larger effect on $p(\theta)$ than $b$ or $k_s$. Interestingly and somewhat counter intuitively, the sensitivity of volumetric soil moisture to a perturbation in the depth of the root zone $d_{rz}$ is much smaller than for an equal perturbation in $\theta_s$ (Figs. 4e and 4j), since the effect of the former occurs through the water balance. However, actual variations in $d_{rz}$ can be expected to be larger than ±10%, both within and between different models.

For the vegetation parameters that directly control ET (LAI, $r_{s,min}$), the effect is rather independent of climate (Figs. 4k and 4l). Because of the additive nature of the canopy and aerodynamic resistance $r_c$ and $r_a$, their individual effect on $p(\theta)$ is smaller than for LAI. Since $r_a \ll r_c$, LAI and $r_{s,min}$ show higher sensitivities. Much larger effects are found in all climates for the parameters $\Delta q$, $\alpha$, $\lambda$ that are directly linked to atmospheric forcing (Figs. 4n–p). As mentioned earlier, not all parameters are equally uncertain in reality. Ideally, the sensitivity should be evaluated with realistic rather than equal perturbations. Figure 5 shows the effect of one of the most uncertain parameters, $k_s$, with a 10% perturbation as compared to a more realistic 50%–200% scenario. In the latter case, the effect on $p(\theta)$ becomes comparable to a 10% uncertainty in $\theta_s$ (Fig. 4e).

With soil moisture being sensitive to certain parameters, this is not necessarily also true for ⟨ET⟩. Figure 6 shows the relative sensitivity $\sigma$ [Eq. (22)] of ⟨ET⟩ to all parameters (again, including forcing). While some (soil) parameters have a profound effect on soil moisture, this effect is not reflected in ET. Only in the transitional climate is there a small relative sensitivity (order ±0.1) of ⟨ET⟩ to some soil parameters ($\theta_c$, $\theta_s$) compared to none for the humid and arid climates. This sensitivity dependence on the climate regime is as expected, since ET will be most significantly affected by soil moisture in the transitional climate (see also Koster et al. 2004). In the humid and transitional climates, ⟨ET⟩ is much more sensitive to (vegetation) parameters that directly determine $ET_{max}$ (LAI, $r_{s,min}$, $\Delta q$). In the arid climate, nearly all precipitation evaporates, resulting in a sensitivity of 1 to changes in $\alpha$ and $\lambda$. In the humid climate, ⟨ET⟩ becomes nearly insensitive to small changes in precipitation characteristics.
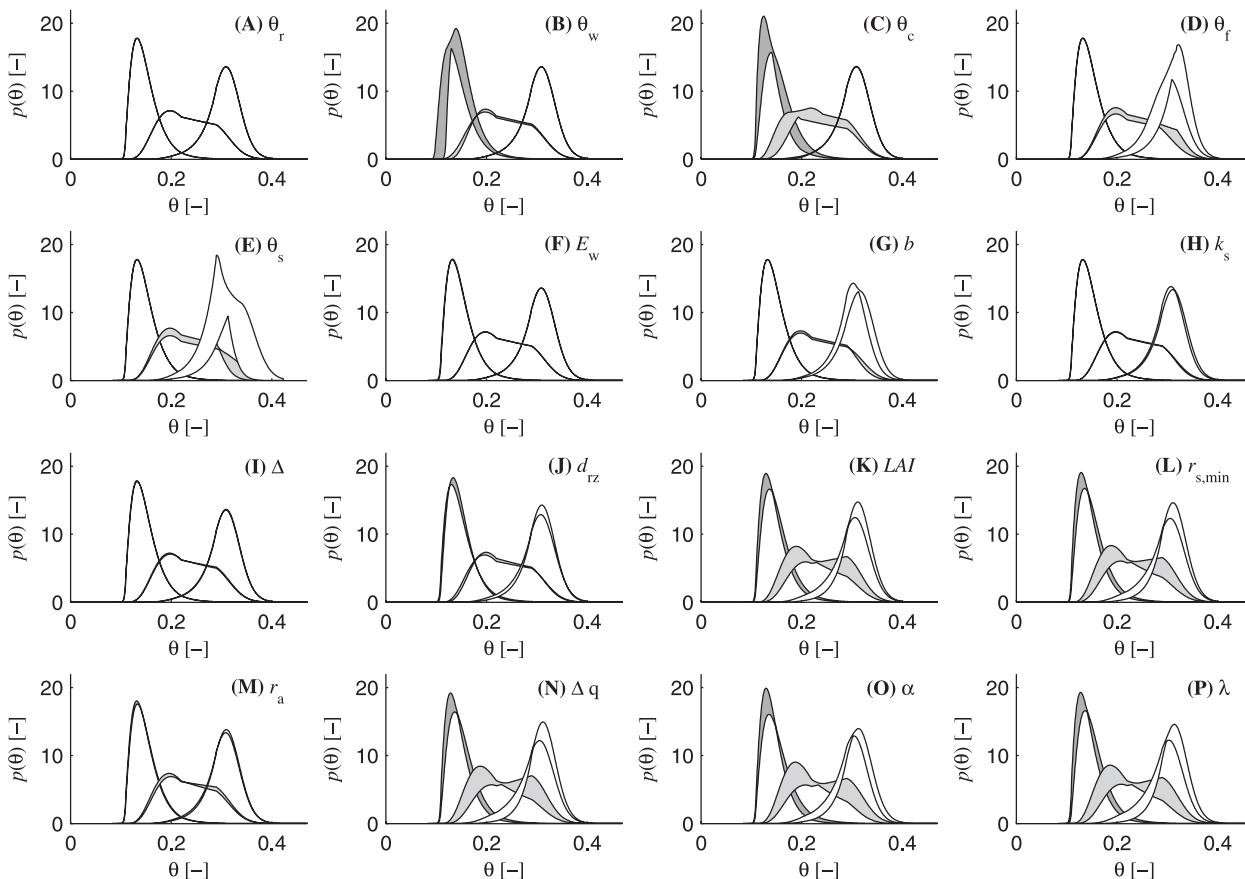
FIG. 4. (a)–(p) Sensitivity of the steady-state soil moisture distribution $p(\theta)$ to its parameters for arid (gray and in the background and left curves), transitional (light gray and the middle curves), and humid (white and in the front and right curves) climates. The filled areas correspond to the outer envelope, which contains all pdfs resulting from perturbing each parameter in a $\pm10\%$ interval. Reference parameters were taken as $\theta_r = 0.08$, $\theta_w = 0.11$, $\theta_c = 0.22$, $\theta_f = 0.29$, $\theta_s = 0.47$, $E_w = 0.2$ mm day$^{-1}$, $b = 6$, $k_s = 400$ mm day$^{-1}$, $\Delta = 0.5$ mm, $d_{rz} = 600$ mm, LAI = 3, $r_{s,min} = 150$ s m$^{-1}$, and $r_a = 10$ s m$^{-1}$. Here, $\Delta q$ was inverted from ET$_{max}$. Values for ET$_{max}$, $\alpha$, and $\lambda$ depend on climate (Table 1).

## b. ELDAS soil parameters

Table 2 lists the soil parameters for different soil types in the ELDAS models. It should be noted that not all models include a distinction between the functional role of $\theta_r$ and $\theta_w$, or between $\theta_c$ and $\theta_f$. In TESSEL, for example, there is no mechanism that allows for drying below $\theta_w$; hence, $\theta_w$ has the same function in the model as $\theta_r$. Because of the small fluxes below $\theta_r$, this distinction does not necessarily have a large effect on either $\theta$ or ET. Large differences in $\theta_w$ are found between the models. For coarse soils, $\theta_w$ in TERRA (0.042) is half of $\theta_w$ in ISBA (0.083). For very fine soils, the difference between TERRA and HTESSEL is even larger: 0.257 versus 0.335. Similar differences are found for $\theta_c$ and $\theta_s$.

All models increase their relevant soil moisture contents from coarse to fine soils, though with different magnitude. For HTESSEL, the difference in $\theta_s$ between

coarse and very fine soils is 0.211; for ISBA, this is only 0.076. Even larger differences are found in $k_s$. For the same soil type, the models often differ over more than one order of magnitude. Similar to the previously discussed parameters, the range in $k_s$ between different
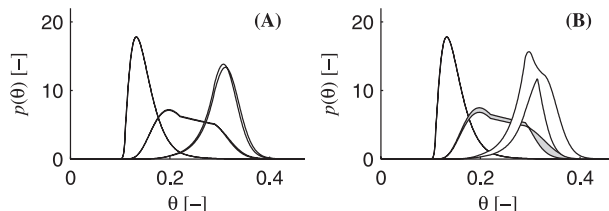


FIG. 5. Sensitivity of the steady-state soil moisture distribution $p(\theta)$ for $k_s$ for arid, transitional, and humid climates using the depiction scheme of Fig. 4: (a) $\pm10\%$ $k_s$ range; (b) Half to double (50%–200%) $k_s$ range. Reference parameters are as in Fig. 4.
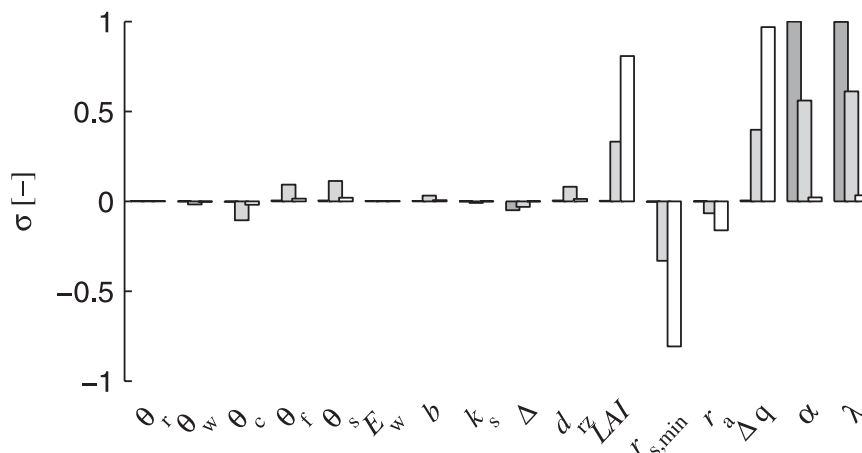
FIG. 6. The relative sensitivity $\sigma$ [Eq. (22)] of average evapotranspiration $\langle ET \rangle$ to model parameters, as in Fig. 4, for the arid, transitional, and humid climates. A sensitivity of 1 means that any relative change in the parameter results in an equal relative change in $\langle ET \rangle$. Reference parameters are as in Fig. 4.

soils in a single model also differs widely. In TERRA, this range is most extreme, with 4138 mm day$^{-1}$ for sand and only 1 mm day$^{-1}$ for clay. In ISBA, this range is much smaller, with 497 mm day$^{-1}$ for sand and 37 mm day$^{-1}$ for clay. This also illustrates the very large range of uncertainty that can be found for certain parameters (since the soil texture of a given model grid point will often lie between typical soil texture classes).

Important to the modeling of soil moisture–limited ET is the moisture availability per unit depth between the wilting point $\theta_w$ and the critical moisture content $\theta_w$. For convenience, this difference $\theta_c - \theta_w$ is also listed in Table 2. Although within any model, the variability of the difference between soil types is limited and the differences between the models are very large. Whereas HTESSEL has differences in the range 0.196–0.250, the differences for ISBA are nearly 3 times smaller, 0.073–0.089. Next, the effect of the different parameters on soil moisture and the water balance components is investigated.

### c. Effect of ELDAS soil parameters

Figure 7 shows the pdfs with ELDAS parameters calculated with Eq. (14) (ISBA parameters) and Eq. (15) (TERRA and HTESSEL parameters). The soil moisture distributions directly reflect the tendency of the soil parameters to increase with finer texture. Compared to our reference model, the ELDAS models all have a large difference $\theta_c - \theta_w$ (see Table 2) in comparison to $\theta_f - \theta_c$. In combination with relatively rapid drainage above $\theta_f$, this leads to a much smaller soil moisture variability (i.e., narrower pdfs) in the humid climate than in the arid climate.

The reference parameters also result in a rather wide pdf for the transitional climate when compared to the humid and arid climates (Fig. 4). For the HTESSEL and ISBA parameters, this behavior is almost absent. The small range over which soil moisture can vary in ISBA causes the pdfs for different climates to largely overlap. For TERRA and HTESSEL, the climate signal in the soil moisture pdfs is much stronger. Even for the same soil type, the soil moisture pdfs between the models sometimes hardly overlap, as is the case for HTESSEL and ISBA. This shows that soil parameters can be a major source of absolute bias when different soil moisture products are to be compared, which has also been identified in previous studies (e.g., Dirmeyer et al. 1999).

As shown before, effects on soil moisture do not necessarily translate into effects on water fluxes. Table 3 lists all average water fluxes that are affected by soil moisture and soil parameters ($\langle ET \rangle$, $\langle Q \rangle$, $\langle R \rangle$) for the arid, transitional, and humid climates. The fluxes that are independent of soil moisture ($\langle P \rangle$, $\langle I \rangle$) are listed in Table 1.

For TERRA and (H)TESSEL in the arid climate, $\langle ET \rangle$ approaches the average infiltration rate $\langle P \rangle - \langle I \rangle = 1.90$ mm day$^{-1}$, and drainage losses are small. Because of the small dynamic range caused by the ISBA parameters, drainage losses are much larger (up to 10% of $\langle ET \rangle$ for sand). In the transitional climate, $\langle ET \rangle$ is highest for all models despite the smaller $ET_{max}$. The $\langle ET \rangle$ tends to be higher for finer soils, especially for peat/ organic soil. The increased precipitation is accompanied by a general increase in $\langle Q \rangle$. There are, however, considerable intermodel differences. TERRA has a slightly higher $\langle ET \rangle$ than TESSEL, most likely due to the higher
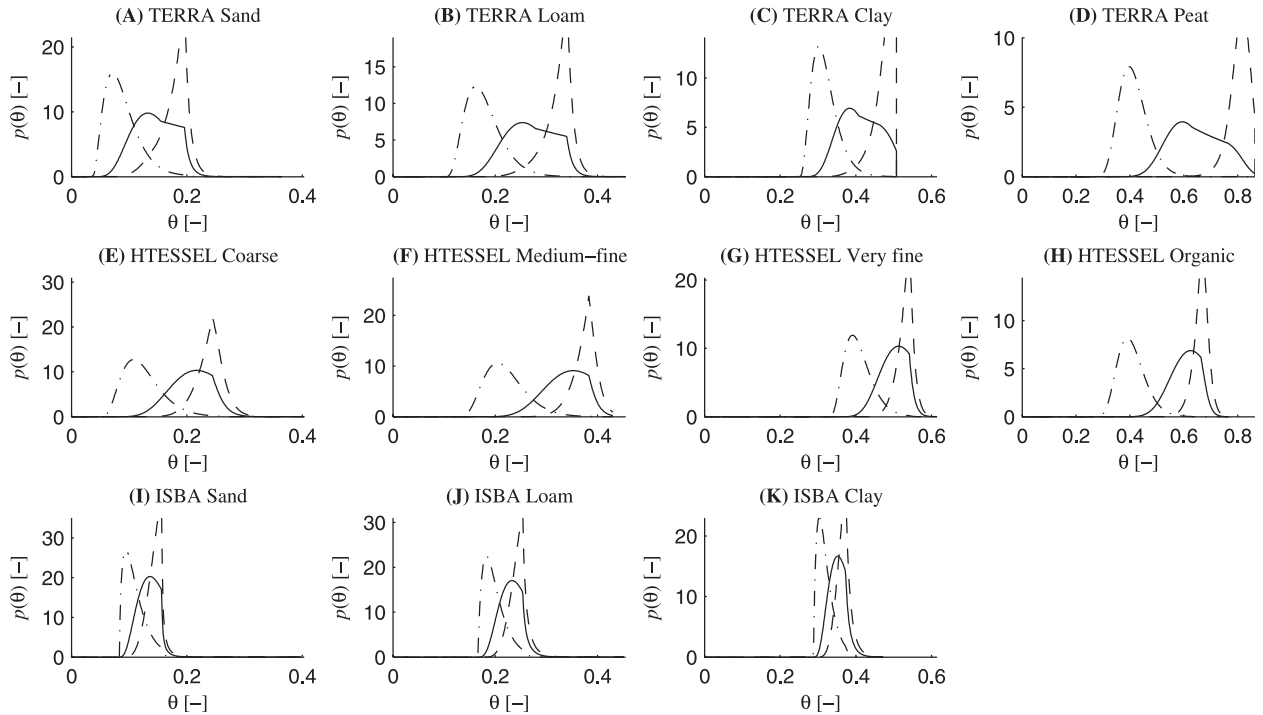
FIG. 7. Steady-state soil moisture distributions $p(\theta)$ with ELDAS parameters for (a)–(k) selected soil types and for arid (dash–dotted), transitional (solid), and humid (dashed) climates. Common parameters: $E_w = 0.2$ mm day$^{-1}$, $\Delta = 0.5$ mm, and $d_{rz} = 600$ mm. For convenience, the same $x$ axis is chosen for similar soil types.

ET above $\theta_c$. Again, the smaller dynamic range in ISBA leads to increased $\langle Q \rangle$ and thus reduced $\langle ET \rangle$ by 10%–20%. In the humid climate, $\langle ET \rangle$ approaches $ET_{max}$ (3.0 mm day$^{-1}$). In (H)TESSEL and ISBA, the more frequent soil moisture reduction on ET (below $\theta_f$ rather than $\theta_c$) leads to smaller $\langle ET \rangle$ (5%–15%) and consequently larger $\langle Q \rangle$. Only for the cases with extremely low $k_s$, $\langle R \rangle$ becomes significant at the cost of $\langle Q \rangle$. In the humid and transitional climates, model differences in $\langle ET \rangle$ are much larger than in the arid climate.

Next, we quantify the effect of the ELDAS parameters in the arid climate using Eqs. (19)–(21). Table 2 also lists the mean soil moisture $\langle \theta \rangle$ for the arid climate. For all models, $\langle \theta \rangle$ increases with finer soil texture, corresponding to the same tendency in the parameters $\theta_w$ and $\theta_c$. For coarse soils, $\langle \theta \rangle$ is very similar; however, the differences in $\theta_c - \theta_w$ nonetheless result in completely different dynamics in terms of Var($\theta$) and Var(ET). For finer soils, both $\langle \theta \rangle$ and $\theta_c - \theta_w$ show large differences between the models, with differences in $\langle \theta \rangle$ of up to 0.07. For loamy soils in HTESSEL and ISBA, $\langle \theta \rangle$ is very similar; however, the large difference in $\theta_c - \theta_w$ results in ISBA having a nearly 3 times larger Var(ET) and a corresponding Var($\theta$) 3 times smaller in comparison to HTESSEL. For clay soils, the difference in $\langle \theta \rangle$ between the models can be as high as 0.09.

## d. Model structure

TERRA differs from the other models not only by its reduction of $\langle ET \rangle$ below $\theta_c$ rather than $\theta_f$ (a parameter difference) but also by the variation of $\theta_c$ depending on

TABLE 3. Effect of ELDAS soil parameters on average soil water fluxes (mm day$^{-1}$) for the soil types in Fig. 7. The accompanying (soil independent) fluxes $\langle P \rangle$ and $\langle I \rangle$ are listed in Table 1, yielding not-average inputs $\langle P \rangle - \langle I \rangle$ of 1.90, 3.80, and 4.76 mm day$^{-1}$ for the three climates, respectively.

| Soil texture | Arid | | | Transitional | | | Humid | | |
|---|---|---|---|---|---|---|---|---|---|
| | $\langle ET \rangle$ | $\langle Q \rangle$ | $\langle R \rangle$ | $\langle ET \rangle$ | $\langle Q \rangle$ | $\langle R \rangle$ | $\langle ET \rangle$ | $\langle Q \rangle$ | $\langle R \rangle$ |
| TERRA parameters | | | | | | | | | |
| Sand | 1.89 | 0.02 | 0.00 | 3.31 | 0.49 | 0.00 | 2.95 | 1.81 | 0.00 |
| Loam | 1.90 | 0.00 | 0.00 | 3.45 | 0.36 | 0.00 | 2.98 | 1.77 | 0.01 |
| Clay | 1.90 | 0.00 | 0.00 | 3.49 | 0.08 | 0.24 | 2.99 | 0.40 | 1.36 |
| Peat | 1.90 | 0.00 | 0.00 | 3.67 | 0.10 | 0.04 | 3.00 | 1.18 | 0.59 |
| HTESSEL parameters | | | | | | | | | |
| Coarse | 1.89 | 0.01 | 0.00 | 3.22 | 0.58 | 0.00 | 2.84 | 1.91 | 0.00 |
| Medium fine | 1.90 | 0.00 | 0.00 | 3.28 | 0.42 | 0.10 | 2.86 | 1.52 | 0.39 |
| Very fine | 1.89 | 0.01 | 0.00 | 3.21 | 0.58 | 0.02 | 2.82 | 1.87 | 0.07 |
| Organic | 1.90 | 0.00 | 0.00 | 3.42 | 0.38 | 0.01 | 2.93 | 1.79 | 0.04 |
| ISBA parameters | | | | | | | | | |
| Sand | 1.74 | 0.16 | 0.00 | 2.70 | 1.11 | 0.00 | 2.48 | 2.28 | 0.00 |
| Loam | 1.81 | 0.10 | 0.00 | 2.86 | 0.94 | 0.00 | 2.61 | 2.15 | 0.00 |
| Clay | 1.81 | 0.09 | 0.00 | 2.90 | 0.90 | 0.01 | 2.64 | 2.09 | 0.02 |
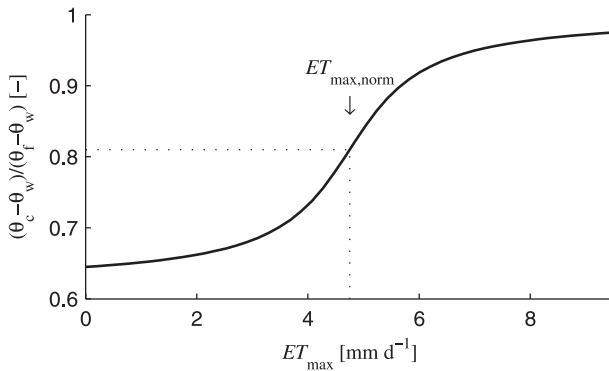
FIG. 8. Dependence of the critical moisture content $\theta_c$ on $ET_{max}$ in TERRA [Eq. (27)].



FIG. 9. The effect of drainage parameterization on the soil moisture distribution $p(\theta)$: 1 indicates linear drainage with the same $k_s$ as nonlinear drainage; 2 is the effective $k_s$ using the approach of Mahfouf and Noilhan (1996); and 3 indicates the closest correspondence between the pdfs for linear and nonlinear drainage when also $\theta_f$ is varied. Inset shows the corresponding minimum in the RMSE between the two pdfs.

$ET_{max}$ [a model structure difference, Eq. (27)]. The question arises of how much the structural difference can add to the difference between the ELDAS parameters. Figure 8 shows Eq. (27). For low $ET_{max}$, the relative critical moisture content approaches 0.65, while for high $ET_{max}$ it approaches 1 (or $\theta_f$). Since in a humid climate $ET_{max}$ is generally low and $\langle ET \rangle \approx ET_{max}$, a lowering of $\theta_c$ will only have a minor effect on $\langle ET \rangle$ and $\theta$. In an arid climate with high $ET_{max}$, a higher $\theta_c$ will affect $\theta$ rather than $\langle ET \rangle$, since $\langle ET \rangle$ is mainly determined by the mean infiltration. In transitional climates, the sensitivity of $\langle ET \rangle$ to $\theta_c$ is highest (Fig. 6) and the effect on $\langle ET \rangle$ should be largest.

Part of the difference between ISBA and (H)TESSEL and TERRA parameters originates from the difference in drainage, that is, Eq. (8) versus Eq. (9). The "effective" saturated hydraulic conductivity $C_3$ was derived under the requirement of the same $e$-folding time for free drainage from saturation (Mahfouf and Noilhan 1996). However, under normal wet conditions, the corresponding soil moisture level $\theta^*$ is almost never reached (Fig. 9). The poor match between the linear and nonlinear drainage does not imply the former to be an incorrect model. With a proper choice of effective parameters, a reasonable fit can be obtained with the nonlinear drainage. Figure 9 also shows the "best fit" pdf obtained by minimizing the RMSE between the pdfs with linear and nonlinear drainage. This leads to a further reduction of $k_s$ to only 20% of its original (physical) value and to an increase in $\theta_f$ by 0.03.

## 4. Discussion and conclusions

In this paper, we analyzed soil parameters of three land surface models used within the ELDAS project, and we evaluated their potential effect on soil moisture and different water balance components. First, it was shown that soil moisture in LSMs is much more sensi-
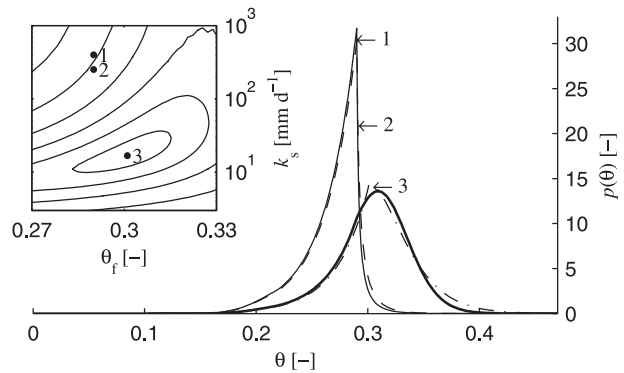
tive to soil parameters than evapotranspiration. The difference between the LSM soil parameters, however, was so large that evapotranspiration was also affected, resulting in differences of more than 10% in evapotranspiration as a result of soil parameters alone. We should note that it is most directly the effect of soil parameters on land fluxes (rather than absolute soil moisture content) that is relevant for coupled models. That models can have highly varying absolute soil moisture values does not necessarily mean that soil moisture dynamics and its effect on evapotranspiration is affected (see also Dirmeyer et al. 1999).

The available moisture content per unit depth and thus the range of soil moisture (which is, as mentioned, more important for the models' behavior than for the absolute soil moisture bounds) differed between the models by up to a factor of 2. The ISBA parameters resulted in a smaller soil moisture range and less evapotranspiration for all soil types in comparison to (H)TESSEL and TERRA. The different behavior of the ISBA parameters can partly be explained by the different drainage parameterization. The linear force–restore drainage formulation in ISBA, when not used in combination with the proper effective field capacity and saturated hydraulic conductivity, results in a much more efficient drainage in comparison to the nonlinear formulation in (H)TESSEL and TERRA. In conclusion, the different soil parameters used in the investigated LSMs can lead to significant volumetric soil moisture biases of up to 0.10 and can cause differences in evapotranspiration of up to 10%.

The parsimonious (i.e., low dimensional) analytical models of the soil water balance are an easy tool used to

investigate sensitivities of soil moisture and water fluxes to primary parameters without using full LSMs with more complex parameter interactions. Despite the simplicity of our model, the results are in line with previous studies on full LSMs. Large sensitivity of soil moisture to soil parameters was also reported by Braun and Schädler (2005). In an intermodel comparison, Koster and Milly (1997) found that ISBA was among the models with the lowest average evapotranspiration, consistent with the low water availability per unit depth discussed here. The dependency of parameter sensitivity to climate conditions that was reported in several studies (e.g., Bastidas et al. 1999; Soet et al. 2000; Kahan et al. 2006) is also well reproduced in the current study. More specifically, our results also agree on the higher sensitivity of evapotranspiration to vegetation parameters in comparison to soil parameters under dry conditions (Kahan et al. 2006). Kato et al. (2007) studied the sensitivity of different parameters of three LSMs used within the Global Land Data Assimilation System (GLDAS) project and also found that evapotranspiration was more sensitive to land cover, while soil moisture was more sensitive to soil characteristics. This is consistent with our Figs. 4 and 6.

While the stochastic soil moisture models can be seen as "generalized" land surface models for the water balance per unit depth, they obviously have their limitations. First, they lack interaction with the atmosphere. In coupled models, the effect of this interaction can be significant (Pitman 1994). Although coupling with the atmosphere will likely result in different sensitivities, high sensitivities to stomatal resistance and leaf area index (among other factors) were also reported by Pitman (1994) for a coupled experiment. Second, the fact that these models treat the unsaturated zone as a single layer makes them incapable of simulating processes, such as infiltration and vertical redistribution that take place on fine temporal scales and require fine vertical and horizontal discretization. For soils with low saturated hydraulic conductivity in arid climates, where infiltration excess runoff is not compensated by saturation excess runoff, the effect on the water balance might be significant. The stochastic soil models used here also lack seasonality in forcing. Since seasonality is an inherent property of most climates, the results should, therefore, be interpreted in a probabilistic manner. For short simulations, the role and sensitivity of parameters might depend more on the initial soil moisture state than on climate. Finally, any LSM grid cell will contain a mixture of different soil types. Different LSMs might determine the representative soil type for the grid cell differently, leading to additional intermodel differences not considered here.

## REFERENCES

Albertson, J. D., and G. Kiely, 2001: On the structure of soil moisture time series in the context of land surface models. *J. Hydrol.,* **243,** 101–119.

Bastidas, L. A., H. V. Gupta, S. Sorooshian, W. J. Shuttleworth, and Z. L. Yang, 1999: Sensitivity analysis of a land surface scheme using multicriteria methods. *J. Geophys. Res.,* **104** (D16), 19 481–19 490.

Betts, A. K., J. H. Ball, M. Bosilovich, P. Viterbo, Y. Zhang, and W. B. Rossow, 2003: Intercomparison of water and energy budgets for five Mississippi subbasins between ECMWF reanalysis (ERA-40) and NASA Data Assimilation Office fvGCM for 1990–1999. *J. Geophys. Res.,* **108** (D16), 8618, doi:10.1029/2002JD003127.

Bogaart, P. W., A. J. Teuling, and P. A. Troch, 2008: A state-dependent parameterization of saturated–unsaturated zone interaction. *Water Resour. Res.,* **44,** W11423, doi:10.1029/2007WR006487.

Bouttier, F., J.-F. Mahfouf, and J. Noilhan, 1993: Sequential assimilation of soil moisture from atmospheric low-level parameters. Part I: Sensitivity and calibration studies. *J. Appl. Meteor.,* **32,** 1335–1351.

Braun, F. J., and G. Schädler, 2005: Comparison of soil hydraulic parameterizations for mesoscale meteorological models. *J. Appl. Meteor.,* **44,** 1116–1132.

Calanca, P., 2004: Interannual variability of summer mean soil moisture conditions in Switzerland during the 20th century: A look using a stochastic soil moisture model. *Water Resour. Res.,* **40,** W12502, doi:10.1029/2004WR003254.

Clapp, R. B., and G. M. Hornberger, 1978: Empirical equations for some soil hydraulic properties. *Water Resour. Res.,* **14,** 601–604.

Crow, W. T., and E. F. Wood, 2002: Impact of soil moisture aggregation on surface energy flux prediction during SGP'97. *Geophys. Res. Lett.,* **29,** 1008, doi:10.1029/2001GL013796.

Denmead, O. T., and R. H. Shaw, 1962: Availability of soil water to plants as affected by soil moisture content and meteorological conditions. *Agron. J.,* **54,** 385–390.

Dirmeyer, P. A., A. J. Dolman, and N. Sato, 1999: The pilot phase of the Global Soil Wetness Project. *Bull. Amer. Meteor. Soc.,* **80,** 851–878.

Douville, H., 2003: Assessing the influence of soil moisture on seasonal climate variability with AGCMs. *J. Hydrometeor.,* **4,** 1044–1066.

——, P. Viterbo, J. Mahfouf, and A. C. M. Beljaars, 2000: Evaluation of the optimum interpolation and nudging techniques for soil moisture analysis using FIFE data. *Mon. Wea. Rev.,* **128,** 1733–1756.

Galantowicz, J. F., D. Entekhabi, and E. G. Njoku, 1999: Tests of sequential data assimilation for retrieving profile soil moisture and temperature from observed L-band radiobrightness. *IEEE Trans. Geosci. Remote Sens., 37,* 1860–1870.

Gutmann, E. D., and E. E. Small, 2006: The effect of soil hydraulic properties vs. soil texture in land surface models. *Geophys. Res. Lett., 32,* L02402, doi:10.1029/2004GL021843.

Heathman, G. C., P. J. Starks, L. R. Ahuja, and T. J. Jackson, 2003: Assimilation of surface soil moisture to estimate profile soil water content. *J. Hydrol., 279,* 1–17.

Ines, A. V. M., and B. P. Mohanty, 2008: Near-surface soil moisture assimilation for quantifying effective soil hydraulic properties under different hydroclimatic conditions. *Vadose Zone J., 7,* 39–52.

Jacobs, C. M. J., and Coauthors, 2008: Evaluation of European Land Data Assimilation System (ELDAS) products using in situ observations. *Tellus, 60A,* 1023–1037.

Jarvis, P. G., 1976: The interpretation of the variations in leaf water potential and stomatal conductance found in canopies in the field. *Philos. Trans. Roy. Soc. London,* **B273,** 593–610.

Kahan, D. S., Y. Xue, and S. J. Allen, 2006: The impact of vegetation and soil parameters in simulations of surface energy and water balance in the semi-arid Sahel: A case study using SEBEX and HAPEX-Sahel data. *J. Hydrol., 320,* 238–259.

Kato, H., M. Rodell, F. Beyrich, H. Cleugh, E. van Gorsel, H. Liu, and T. P. Meyers, 2007: Sensitivity of land surface simulations to model physics, land characteristics, and forcings, at four CEOP sites. *J. Meteor. Soc. Japan, 85A,* 187–204.

Koster, R. D., and M. J. Suarez, 1996: The influence of land surface moisture retention on precipitation statistics. *J. Climate, 9,* 2551–2567.

——, and P. C. D. Milly, 1997: The interplay between transpiration and runoff formulations in land surface schemes used with atmospheric models. *J. Climate, 10,* 1578–1591.

——, and M. J. Suarez, 2001: Soil moisture memory in climate models. *J. Hydrometeor., 2,* 558–570.

——, and Coauthors, 2004: Regions of strong coupling between soil moisture and precipitation. *Science, 305,* 1138–1140.

Laio, F., A. Porporato, L. Ridolfi, and I. Rodríguez-Iturbe, 2001: Plants in water-controlled ecosystems: Active role in hydrologic processes and response to water stress. II: Probabilistic soil moisture dynamics. *Adv. Water Resour., 24,* 707–723.

Liang, X., and J. Guo, 2003: Intercomparison of land-surface parameterization schemes: Sensitivity of surface energy and water fluxes to model parameters. *J. Hydrol., 279,* 182–209.

Lohmann, D., and E. F. Wood, 2003: Timescales of land surface evapotranspiration response in the PILPS phase 2(c). *Global Planet. Change, 38,* 81–91.

Mahfouf, J.-F., 1991: Analysis of soil moisture from near-surface parameters: A feasibility study. *J. Appl. Meteor., 30,* 1534–1547.

——, and J. Noilhan, 1996: Inclusion of gravitational drainage in a land surface scheme based on the force–restore method. *J. Appl. Meteor., 35,* 987–992.

Manabe, S., 1969: Climate and the ocean circulation. I: The atmospheric circulation and the hydrology of the earth's surface. *Mon. Wea. Rev., 97,* 739–774.

Miller, G. R., D. B. Baldocchi, B. E. Law, and T. Meyers, 2007: An analysis of soil moisture dynamics using multi-year data from a network of micrometeorological observation sites. *Adv. Water Resour., 30,* 1065–1081.

Noilhan, J., and J.-F. Mahfouf, 1996: The ISBA land surface parameterisation scheme. *Global Planet. Change, 13,* 145–159.

Pitman, A. J., 1994: Assessing the sensitivity of a land-surface scheme to the parameter values using a single column model. *J. Climate, 7,* 1856–1869.

Reichle, R. H., and R. D. Koster, 2005: Global assimilation of satellite surface soil moisture retrievals into the NASA Catchment land surface model. *Geophys. Res. Lett., 32,* L02404, doi:10.1029/2004GL021700.

Rhodin, A., F. Kucharski, U. Callies, D. P. Eppel, and W. Wergen, 1999: Variational analysis of effective soil moisture from screen-level atmospheric parameters: Application to a short-range weather forecast model. *Quart. J. Roy. Meteor. Soc.,* **125,** 2427–2448.

Richter, H., A. W. Western, and F. H. S. Chiew, 2004: The effect of soil and vegetation parameters in the ECMWF land surface scheme. *J. Hydrometeor., 5,* 1131–1146.

Rodríguez-Iturbe, I., and A. Porporato, 2004: *Ecohydrology of Water-Controlled Ecosystems.* Cambridge University Press, 442 pp.

——, ——, L. Ridolfi, V. Isham, and D. R. Cox, 1999: Probabilistic modelling of water balance at a point: The role of climate, soil and vegetation. *Proc. Roy. Soc. London,* **A455,** 3789–3805.

Schenk, H. J., and R. B. Jackson, 2002: The global biogeography of roots. *Ecol. Monogr., 72,* 311–328.

Schuurmans, J. M., P. A. Troch, A. A. Veldhuizen, W. G. M. Bastiaanssen, and M. F. P. Bierkens, 2003: Assimilation of remotely sensed latent heat flux in a distributed hydrological model. *Adv. Water Resour., 26,* 151–159.

Sellers, P. J., and Coauthors, 1997: Modeling the exchanges of energy, water, and carbon between continents and the atmosphere. *Science, 275,* 502–509.

——, M. J. Fennessy, and R. E. Dickinson, 2007: A numerical approach to calculating soil wetness and evapotranspiration over large grid areas. *J. Geophys. Res., 112,* D18106, doi:10.1029/2007JD008781.

Seneviratne, S. I., P. Viterbo, D. Lüthi, and C. Schär, 2004: Inferring changes in terrestrial water storage using ERA-40 reanalysis data: The Mississippi River basin. *J. Climate, 17,* 2039–2057.

——, D. Lüthi, M. Litschi, and C. Schär, 2006a: Land–atmosphere coupling and climate change in Europe. *Nature,* **443,** 205–209.

——, and Coauthors, 2006b: Soil moisture memory in AGCM simulations: Analysis of Global Land–Atmosphere Coupling Experiment (GLACE) data. *J. Hydrometeor., 7,* 1090–1112.

Seuffert, G., H. Wilker, P. Viterbo, J.-F. Mahfouf, M. Drusch, and J.-C. Calvet, 2003: Soil moisture analysis combining screen-level parameters and microwave brightness temperature: A test with field data. *Geophys. Res. Lett., 30,* 1498, doi:10.1029/2003GL017128.

Soet, M., and J. N. M. Stricker, 2003: Functional behaviour of pedotransfer functions in soil water flow simulation. *Hydrol. Processes, 17,* 1659–1670.

——, R. J. Ronda, J. N. M. Stricker, and A. J. Dolman, 2000: Land surface scheme conceptualisation and parameter values for three sites with contrasting soils and climate. *Hydrol. Earth Syst. Sci., 4,* 283–294.

Teuling, A. J., R. Uijlenhoet, and P. A. Troch, 2005: On bimodality in warm season soil moisture observations. *Geophys. Res. Lett., 32,* L13402, doi:10.1029/2005GL023223.

——, S. I. Seneviratne, C. Williams, and P. A. Troch, 2006: Observed timescales of evapotranspiration response to soil

moisture. *Geophys. Res. Lett.,* **33,** L23403, doi:10.1029/2006GL028178.

——, R. Uijlenhoet, R. Hurkmans, O. Merlin, R. Panciera, J. P. Walker, and P. A. Troch, 2007: Dry-end surface soil moisture variability during NAFE'06. *Geophys. Res. Lett.,* **34,** L17402, doi:10.1029/2007GL031001.

van den Hurk, B., W. G. M. Bastiaanssen, H. Pelgrum, and E. van Meijgaard, 1997: A new methodology for assimilation of initial soil moisture fields in weather prediction models using Meteosat and NOAA data. *J. Appl. Meteor.,* **36,** 1271–1283.

——, P. Viterbo, A. C. M. Beljaars, and A. K. Betts, 2000: Offline validation of the ERA-40 surface scheme. ECMWF Tech. Rep. 295, 42 pp.

——, J. Ettema, and P. Viterbo, 2008: Analysis of soil moisture changes in Europe during a single growing season in a new ECMWF soil moisture assimilation system. *J. Hydrometeor.,* **9,** 116–131.

Viterbo, P., and A. C. M. Beljaars, 1995: An improved land surface parameterization scheme in the ECMWF model and its validation. *J. Climate,* **8,** 2716–2748.